Radiocarbon, Vol 61, Nr 6, 2019, p 2003–2017 DOI:10.1017/RDC.2019.138
Selected Papers from the 23rd International Radiocarbon Conference, Trondheim, Norway, 17–22 June, 2018

δ^{13}C VALUES OF WOOD AND CHARCOAL REVEAL BROAD ISOTOPIC RANGES AT THE BASE OF THE FOOD WEB

Bente Philippsen[1,2]* • Jesper Olsen[1] • Søren A Sørensen[2] • Bjørnar Måge[2]

[1]Aarhus AMS Centre, Department of Physics and Astronomy and Centre for Urban Network Evolutions (UrbNet), Aarhus University, Denmark
[2]Museum Lolland-Falster, Rødbyhavn, Denmark

ABSTRACT. The aim of this study is to investigate the range, the degree of variability, and a possible time or species dependence of wood and charcoal δ^{13}C values within one small study area. To achieve this, we used δ^{13}C and ^{14}C determinations of more than 400 archaeological samples from a ca. 300 ha area in Denmark, spanning 5000 years and covering several different species. The δ^{13}C values of the wood and charcoal range from −32.8‰ to −21.2‰. We found no time-dependence of wood and charcoal δ^{13}C values, neither in general nor within one species. The mean δ^{13}C of all wood samples is −28.5‰, while the means of individual species range from −30.6‰ to −26.3‰. The mean of all charcoal samples is −25.7‰, with the means of individual species ranging from −28.1‰ to −24.3‰. The wood δ^{13}C values can be used to infer the possible range of plant δ^{13}C values, which otherwise are not available. They imply that a high degree of variability can be expected at the base of the food chain. This is relevant for palaeodietary studies that rely on the measurement of baseline isotope values.

KEYWORDS: δ^{13}C, charcoal, isotope baseline, radiocarbon, wood.

INTRODUCTION

Heaton (1999) provides a useful review of the processes influencing plant C-isotope composition. It has long been known that there exists considerable variation in the δ^{13}C values of plants (Wickman 1952; Craig 1953). The δ^{13}C values in plant organic matter depend on two main factors, the δ^{13}C value of the source CO_2 and the fractionation during the processes related to CO_2 uptake and photosynthesis. These two main factors depend on a series of environmental and location-specific parameters, which are summarized below.

The δ^{13}C values of the CO_2 in the global atmosphere vary with time (see Ferrio et al. 2005 for a smoothed curve) and are modified by local variations, such as decreased δ^{13}C values at the bottom of dense forests due to respired CO_2 (the so-called canopy effect, see Vogel 1978; Medina and Minchin 1980; van der Merwe and Medina 1991). The canopy effect contributes to lowered δ^{13}C values in young trees (the so-called juvenile effect), but cannot explain it fully, as the juvenile effect also occurs in open forests (Francey and Farquhar 1982). Ancillary factors could be shading, nutrient deficiency, a decreasing contribution from bark photosynthesis as the tree matures, or changes in the hydraulic conductivity (Francey and Farquhar 1982; McCarroll and Loader 2004).

Fractionation during CO_2 uptake and fixation can be linked to environmental and climatic factors. The two factors that influence fractionation between atmospheric CO_2 and wood are the stomatal conductance of the leaves and the photosynthetic rate, whereby in both the uptake of CO_2 and in its incorporation into the first photosynthetic products, ^{12}C is favored (Park and Epstein 1960). These processes and thus the fractionation can be affected by factors such as water availability, temperature and irradiance (Stuiver and Braziunas 1987; Van de Water et al. 2002; McCarroll and Loader 2004). In the case of water stress, for example, the stomata are constricted reducing the stomatal conductance of CO_2, which in turn reduces discrimination against ^{13}C and thus causing higher δ^{13}C values (McCarroll and Loader 2004; Fiorentino et al. 2014). This has been observed in a

*Corresponding author. Email: bphilipp@phys.au.dk.

variety of species, but especially frequently in arid environments (McCarroll and Loader 2004; Fiorentino et al. 2014; Caracuta et al. 2016).

Several studies have identified a correlation of $\delta^{13}C$ values with summer temperatures, however, this is likely an indirect relation because "hot" summers and drought risk are often correlated (McCarroll and Loader 2004). Another indirect relation could exist between $\delta^{13}C$ values and elevation (Van de Water et al. 2002). In temperate regions, such as Denmark, where commonly no single climate factor limits plant or tree growth, interpretations of $\delta^{13}C$ values are complex (Loader et al. 2008; Young et al. 2012a). $\delta^{13}C$ mainly reflects intracellular CO_2 concentration and hence the rate at which CO_2 is replenished and removed by photosynthesis. Where water stress is low, the photosynthetic rate should dominate (McCarroll and Loader 2004). Recent studies suggest that $\delta^{13}C$ in trees growing close to their latitudinal or altitudinal limits is likely to correlate with measured climate variables such as temperature or sunshine (summer hours of bright sunshine)/cloud cover (Young et al. 2010, 2012b; Gagen et al. 2011; Hafner et al. 2011). Large $\delta^{13}C$ ranges have been measured in modern trees, such as ca. 7‰ in different species of angiosperms (Poole and Bergen 2006). Conifers (gymnosperms) are usually more enriched in $\delta^{13}C$ but are not considered in this study. This study focuses on the variation within and between species and on a local level. All samples analyzed here derive from a site on the south coast of the Danish island of Lolland, from an area of only ca. 300 ha. Due to sea level rise after the last glaciation and the low elevation (the diked area lies 0.5–1 m below sea level today), the site has seen substantial environmental change, as will be detailed below in the site description. One objective of this study is thus to test whether the environmental changes are recorded as $\delta^{13}C$ changes in the wood samples.

The samples used in this study were all radiocarbon dated to provide a chronology for the site. In addition, we measured the $\delta^{13}C$ values of those samples by offline mass spectrometry. We analyzed both uncharred wood and charcoal. As charcoal is the result of the incomplete combustion of wood, fractionation could occur and lead to differences in $\delta^{13}C$ values between wood and charcoal. According to some studies, there are no significant changes in the $\delta^{13}C$ values of wood or plant parts in general due to charring (Leavitt et al. 1982; DeNiro and Hastorf 1985; Hastorf and DeNiro 1985; Marino and DeNiro 1987; Turekian et al. 1998). In other cases, $\delta^{13}C$ decreases with higher carbonization temperature (Ascough et al. 2008), while there is a significant increase in C% (Ferrio et al. 2006). However, carbonizing grass epidermis samples resulted in a ^{13}C-enrichment of 1.0±1.6‰ (Beuning and Scott 2002). An overview of different studies with examples of ^{13}C-enrichment and -depletion is provided by Ascough et al. (2008). It has also been reported that the climatic signal recorded by $\delta^{13}C$ in wood is unaffected by carbonization (Vignola et al. 2018) and that in cases with significant $\delta^{13}C$ shifts, a correction using the measured C% can be applied (Ferrio et al. 2006).

The objective of this study is to analyze the $\delta^{13}C$ values of radiocarbon-dated wood and charcoal samples from the small study area during a period of environmental changes, to assess the degree of variability of the $\delta^{13}C$ values, to study the fractionation during carbonization, to detect possible temporal trends that could be connected to environmental changes, and to examine whether the $\delta^{13}C$ values depend on the tree species, or on the age of the tree/branch. The $\delta^{13}C$ values measured on wood and charcoal could be a proxy for the general variability of plant $\delta^{13}C$ values. As plants are at the base of the food chain, this could be relevant for palaeodietary studies.

https://doi.org/10.1017/RDC.2019.138 Published online by Cambridge University Press

STUDY SITE

Prior to the construction of the planned tunnel through the Fehmarn Belt, between the Danish island of Lolland and the German island of Fehmarn, an area of about 300 hectares, of which 187 ha are former seabed, was examined archaeologically (Sørensen 2016). At the time of writing, the excavations are still ongoing. The study area lies behind a dike constructed at the end of the 19th century in a flat coastal landscape. Hidden below up to 3.5-m-thick layers of sand, the original uneven moraine surface can be found. The former coastal landscape looked quite different than today's and comprised fjords, lagoons and islands. The earliest evidence of human occupation in the study area, fragments of cremated bones found in connection with flint artifacts, are radiocarbon dated to 10,000 BP (Philippsen 2018). During that time, the relative sea level was much lower than today. The study area was initially a forested and hilly area with two hollows. However, the study area was subsequently affected by the rising eustatic sea level after the end of the last glaciation. The interplay between isostatic land rise and eustatic sea level rise caused a complex history of relative sea level changes. From ca. 5000 cal BC, the rising relative sea level caused the groundwater table in the study area to rise, and the hollows became marshy and filled with reed-beds. As the relative sea level continued to rise, the area was inundated, forming two small bays surrounded by reed beds. Later, the peninsula between the bays was inundated as well. The bays were in periods partly cut off from the sea by sand spits, forming a lagoon-like environment. In about 4000 cal BC, the relative sea level rise stopped. The lowest relative sea level was recorded in our excavations to ca. 2.5–3 m below the modern Danish sea level reference (Philippsen 2018). At lower relative sea levels, the entire study area was situated on dry land, making sea level reconstructions for this area impossible. The thick sand deposits covering these layers were probably deposited in connection with falling relative sea levels in the late Holocene. A preliminary relative sea level curve can be found in Philippsen (2018). Both the sea level curve and palaeoenvironmental reconstructions will be refined as the excavations are proceeding.

Similar stratigraphic sequences are observed in large parts of the study area: at the bottom the blue moraine clay, covered with the remains of soil formation in the forested landscape, and overlain by reed peat and finally marine gyttja. These time-transgressive sequences cannot be used for absolute or even relative dating of the artifacts and constructions unearthed in the excavations. Therefore, radiometric dating is crucial for understanding the prehistory of the study area. Waterlogged peat and gyttja deposits provide excellent preservation conditions for organic matter, so there is no lack of datable organic material.

METHODS

The wood and charcoal samples derive from 21 excavation fields within the 300-ha study area on the south coast of the island of Lolland (Figure 1). The wood samples are from stationary fishing devices (fish weirs) and artifacts such as ax handles, spears, bows, arrows, leisters, paddles, and boats, all of which had been lost or were ritually deposited in the shallow water of the former lagoons. The charcoal samples are from fireplaces (especially the oldest samples) or from cooking pits (especially the youngest samples). The samples were chosen for radiocarbon dating based on their archaeological significance, and not targeted at a pure $\delta^{13}C$ study.

Wood and charcoal samples were species-identified by specialists from Moesgård Museum, Højbjerg, Denmark and the National Museum, Copenhagen, Denmark, by microscopic

https://doi.org/10.1017/RDC.2019.138 Published online by Cambridge University Press

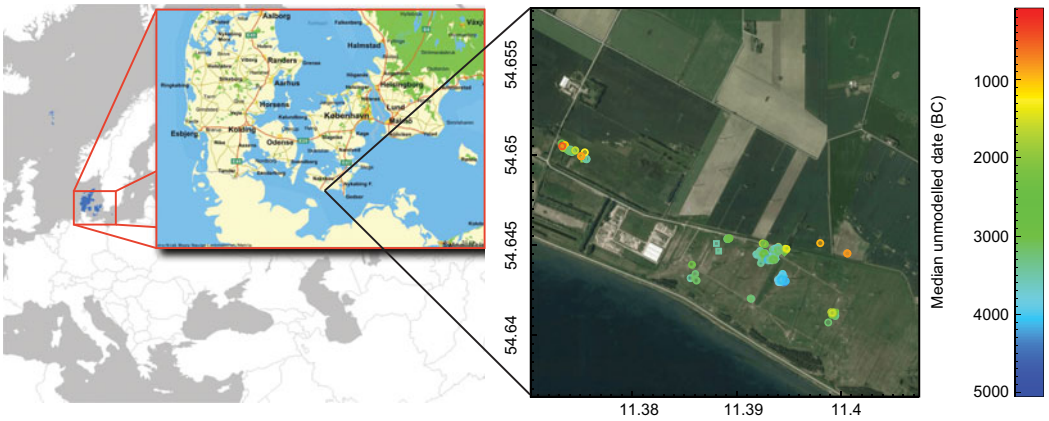

Figure 1 Map of the study area (left side, from www.krak.dk) and sample locations and radiocarbon dates of wooden artifacts plotted on an aerial photo of the site (right side), made with OxCal 4.3 and the calibration curve IntCal13 (Bronk Ramsey 2009; Reimer et al. 2013).

examination of fresh cuts through the samples. The samples were pretreated with a standard ABA treatment: 1M HCl for 1 hr, 1M NaOH for 3 hr (with renewed NaOH if necessary to remove all humics), both at 80°C, and finally 1M HCl overnight at room temperature to remove any CO_2 absorbed during the NaOH treatment. Samples were oven-dried at 80°C, ca. 2 mg weighed out into pre-cleaned quartz tubes containing approximately 200 mg of CuO, evacuated and flame-sealed. Samples were combusted by heating those tubes to 900°C for 3 hr. The resulting CO_2 was isolated cryogenically and reduced to pure carbon (graphite) with the H_2 graphitization method, using Fe as catalyst and $MgClO_4$ to absorb the water forming in the reaction (Vogel et al. 1984; Santos et al. 2007). The samples were radiocarbon dated using the HVE 1MV tandetron accelerator AMS system at the Aarhus AMS Centre (Olsen et al. 2016). Radiocarbon dates are reported as uncalibrated radiocarbon ages BP normalized to −25‰ according to international convention using online $^{13}C/^{12}C$ ratios (Stuiver and Polach 1977). For the figures, we chose to use uncalibrated dates for practical reasons. Our conclusions would not be different if we had used calibrated dates. However, plotting the dates is much easier for radiocarbon dates with a mean and a standard deviation, instead of calibrated dates, where e.g. a probability distribution with two peaks would be represented misleadingly by only the main or median value and standard deviation.

$\delta^{13}C$ was measured on sub-samples weighing ca. 0.25 mg using a continuous-flow IsoPrime IRMS coupled to an Elementar PyroCube elemental analyzer at the Aarhus AMS Centre. An in-house gelatine standard "Gel-A" was used as primary standard yielding ±0.2‰ for carbon analysis. Secondary in-house and international standards were used to check the normalization to the VPDB scale.

All statistical analysis was performed using MatLab, version R2018b. The errors on the linear fit in Figure 4C and D are estimated using a Bootstrap method with 5000 iterations. Figure 3 and Supplementary Figure 2 are computed using the BoxPlot function. The average values in Figure 2 are calculated using a moving window with a size of 100 or 250 ^{14}C years, which is stepped by 25 ^{14}C years in the interval from 2000 to 7000 ^{14}C years. A minimum of 5 data points is required for an average value to be computed. The error on the running mean value is estimated using the standard deviation divided by the square root of the number of data points.

https://doi.org/10.1017/RDC.2019.138 Published online by Cambridge University Press

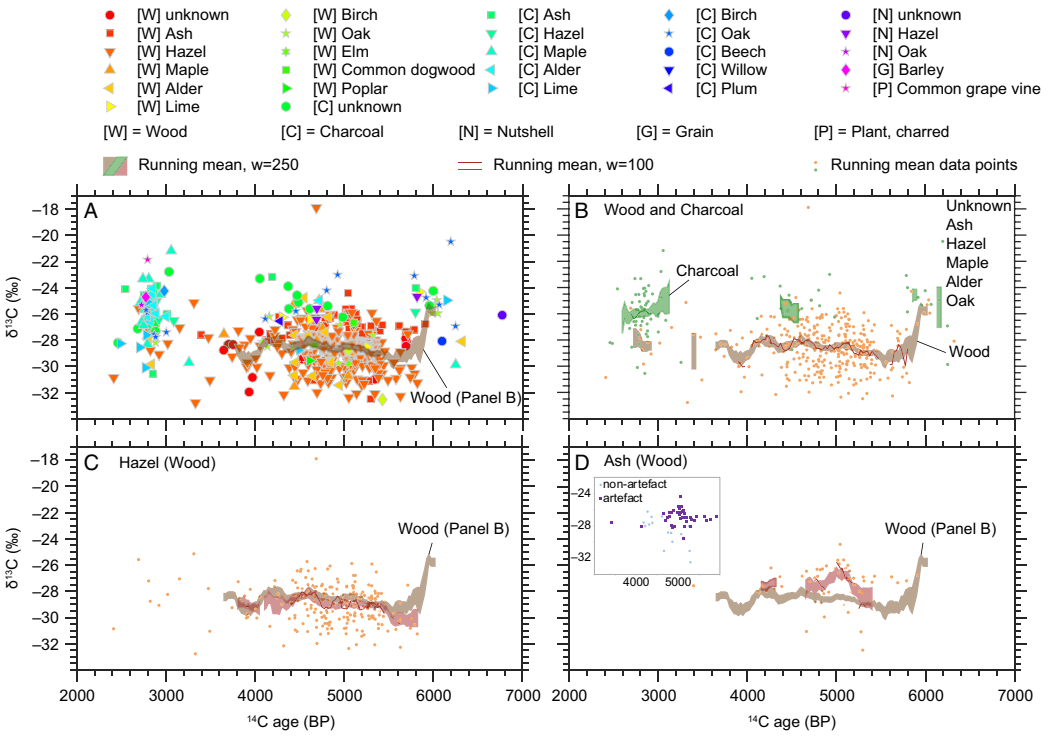

Figure 2 ^{14}C ages (BP) and $\delta^{13}C$ values (‰ VPDB) of wood and charcoal samples from the study area with running means of the charcoal and wood data. Panel A shows all data, panel B differentiates between charcoal and wood, panels C and D show the wood $\delta^{13}C$ values of the two most numerous species with their running means (red) on the background of the running mean of all wood samples (brown). An insert within panel D displays the ash wood $\delta^{13}C$ values of artifacts (such as spears) versus non-artifacts (such as branches used in fish-weirs).

RESULTS

The whole range of $\delta^{13}C$ values and radiocarbon ages is displayed in Figure 2. In Table 1, Figure 3 and Figure 4, the results are shown by species and material. Further information is displayed in two online supplementary figures—the $\delta^{13}C$ values in relation to ^{14}C age and carbon fraction for individual species in Supplementary Figure 1, and a comparison of carbon fraction and $\delta^{13}C$ value of samples from artifacts (i.e., tools such as ax handles, spears, leister prongs, bows and arrows and boats that could have been brought to the site from farther away) versus samples such as firewood or branches for fish weirs, that would have been collected and used locally. As the measured ^{14}C ages did not disagree with the ages expected on the background of the archaeological and stratigraphic information available, we consider the risk of post-depositional contamination affecting the $^{14}C/^{12}C$ and $^{13}C/^{12}C$ ratios to be minimal.

Figure 3 shows carbon fraction and $\delta^{13}C$ value by material and species. Figure 4 is composed of several plots: Panels A and B are histograms of carbon fraction and $\delta^{13}C$ values of all samples. Panels C and D show $\delta^{13}C$ values of the individual samples grouped by the age of the branch/tree when it was cut, where "young" refers to small twigs with 2–7 year rings, "medium" to all bigger branches or artifacts made thereof, and "old" to tree stumps or trunks or artifacts made from those. Panel E shows the difference between wood and charcoal by species.

https://doi.org/10.1017/RDC.2019.138 Published online by Cambridge University Press

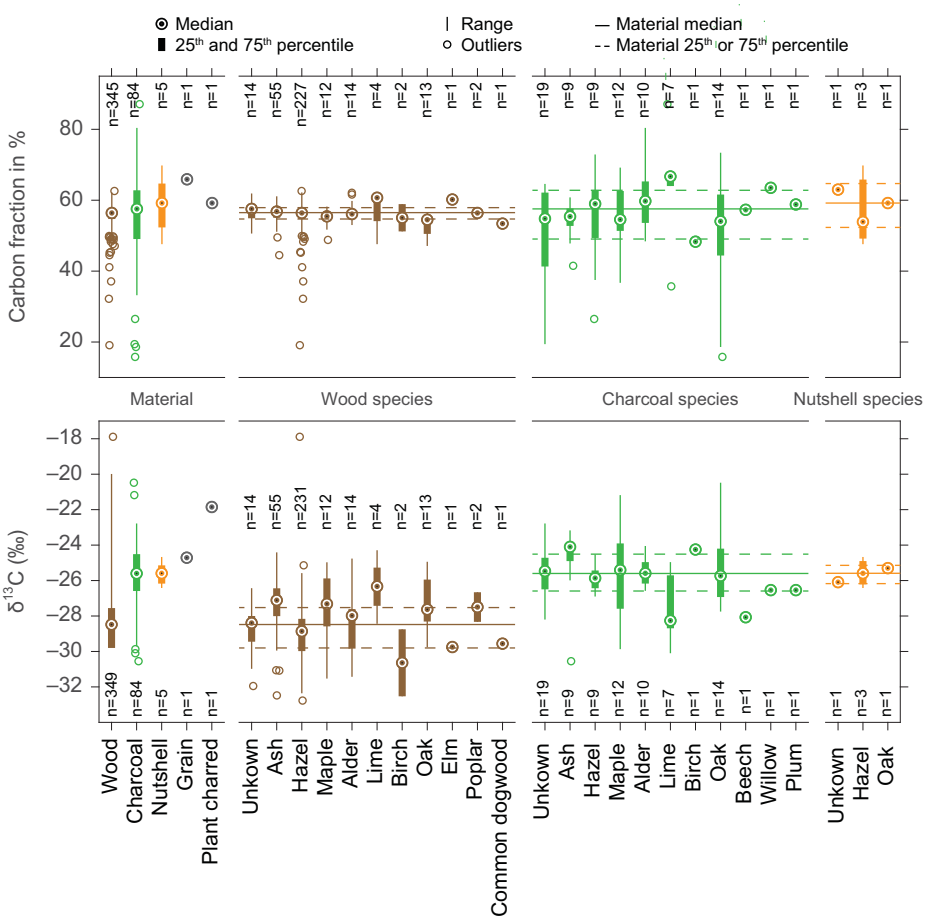

Figure 3 Box plots of the carbon fraction and $\delta^{13}C$ values of the wood and charcoal samples of this study, also per species.

Figure 2 shows that the $\delta^{13}C$ values span a range of more than 11‰, when one outlier of −17.9‰ is excluded. Not all periods are equally represented, for example, there is a relative lack of data from the period 4000–3000 BP. The bulk of data between 5500 and 4500 BP derives from excavations of waterlogged sites, many of them from fish weirs and settlement refuse that was deposited in shallow water. Therefore, many wood samples are preserved from this period. Another cluster of data from 3000 to 2500 BP originates from dryland excavations where only charcoal, and not wood, was well preserved. This period is therefore dominated by charcoal samples. This could explain the slightly higher $\delta^{13}C$ values of the younger period. The running mean of all wood samples shows a decrease of ca. 2‰ just after 6000 BP and only small fluctuations thereafter (Figure 2). The running mean of the hazel $\delta^{13}C$ values increases slightly between 5500 and 4500 BP, while the ash $\delta^{13}C$ values peak around 5000 BP.

Table 1, Figure 3, and Figure 4E show that our charcoal samples tend to be more enriched in $\delta^{13}C$ than wood. This could be caused by the preferential loss of the lighter carbon isotope (^{12}C) during combustion of the volatile components of wood. The differences between wood and charcoal for the different species are summarized in Supplementary Table 1.

https://doi.org/10.1017/RDC.2019.138 Published online by Cambridge University Press

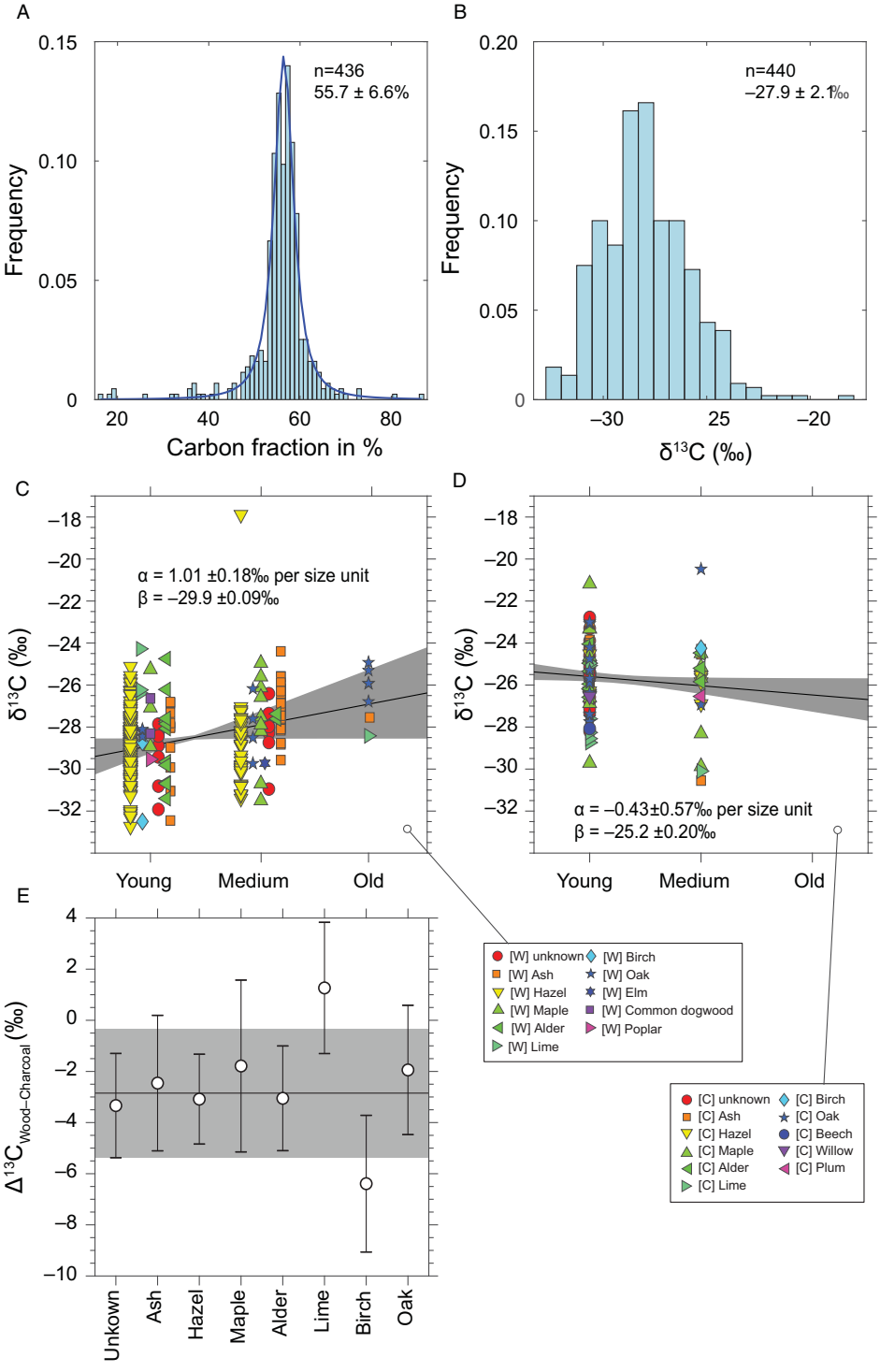

Figure 4 Histograms of A) the carbon fraction and B) the $\delta^{13}C$ values of all samples, C) $\delta^{13}C$ values of the wood and D) of the charcoal species arranged by age of the twig/branch/trunk; E) average $\delta^{13}C$ difference between charcoal and wood per species (the line and shaded area show the average and standard deviation of all samples).

https://doi.org/10.1017/RDC.2019.138 Published online by Cambridge University Press

Table 1 Carbon fraction and $\delta^{13}C$ values (range, average, median and standard deviation) for 440 wood and charcoal samples of this study. $\delta^{13}C$-^{14}C scatter plots and $\delta^{13}C$-histograms of the most abundant species and of unidentified samples are displayed in Supplementary Figure 1, the $\delta^{13}C$ averages and standard deviations (box plots) of all species are shown in Figure 3.

			Carbon fraction in (%)				$\delta^{13}C$ (‰ VPDB)		
Material/species	A	n	μ ± σ (median)	25th–75th percentile	Min–max	n	μ ± σ (median)	25th–75th percentile	min–max
Wood	79.3%	345	55.8 ± 3.9 (56.4)	57.8–57.8	19.1–62.6	349	−28.5 ± 1.7 (−28.5)	−27.6–−27.6	−32.8–−17.9
Unknown	3.2%	14	56.9 ± 2.9 (57.5)	58.3–58.3	50.6–61.9	14	−28.8 ± 1.5 (−28.4)	−28.0–−28.0	−31.9–−26.4
Ash	12.4%	55	56.2 ± 2.8 (56.8)	57.9–57.9	44.5–61.1	55	−27.4 ± 1.4 (−27.1)	−26.4–−26.4	−32.5–−24.4
Hazel	52.5%	227	55.7 ± 4.2 (56.4)	57.8–57.8	19.1–62.6	231	−28.9 ± 1.6 (−28.9)	−28.2–−28.2	−32.8–−17.9
Maple	2.9%	12	55.0 ± 2.6 (55.5)	56.5–56.5	48.8–58.2	12	−27.5 ± 2.1 (−27.3)	−25.9–−25.9	−31.5–−25.0
Alder	3.2%	14	56.7 ± 2.8 (56.1)	57.4–57.4	53.0–62.1	14	−28.5 ± 1.9 (−28.0)	−27.6–−27.6	−31.4–−24.8
Lime	0.9%	4	57.7 ± 6.8 (60.7)	61.3–61.3	47.6–61.9	4	−26.3 ± 1.7 (−26.3)	−25.3–−25.3	−28.4–−24.3
Birch	0.5%	2	55.0 ± 5.4 (55.0)	58.9–58.9	51.2–58.9	2	−30.6 ± 2.7 (−30.6)	−28.8–−28.8	−32.5–−28.8
Oak	2.9%	13	52.9 ± 2.9 (54.5)	54.7–54.7	47.1–56.4	13	−27.2 ± 1.5 (−27.6)	−25.9–−25.9	−29.8–−24.9
Elm	0.2%	1	60.2 ± 0.0 (60.2)	60.2–60.2	60.2–60.2	1	−29.8 ± 0.0 (−29.8)	−29.8–−29.8	−29.8–−29.8
Common dogwood	0.5%	2	56.4 ± 2.0 (56.4)	57.8–57.8	55.0–57.8	2	−27.5 ± 1.2 (−27.5)	−26.7–−26.7	−28.3–−26.7
Poplar	0.2%	1	53.4 ± 0.0 (53.4)	53.4–53.4	53.4–53.4	1	−29.6 ± 0.0 (−29.6)	−29.6–29.6	−29.6–−29.6
Charcoal	19.1%	84	54.9 ± 12.7 (57.5)	62.8–62.8	15.8–87.1	84	−25.7 ± 1.8 (−25.6)	−24.5–−24.5	−30.6–−20.5
Unknown	4.3%	19	50.9 ± 12.9 (54.8)	62.2–62.2	19.4–64.6	19	−25.5 ± 1.4 (−25.5)	−24.7–−24.7	−28.2–−22.8
Ash	2.0%	9	54.1 ± 5.9 (55.4)	57.7–57.7	41.5–60.8	9	−25.0 ± 2.2 (−24.1)	−24.0–−24.0	−30.6–−23.2
Hazel	2.0%	9	54.9 ± 14.3 (59.0)	62.9–62.9	26.5–72.9	9	−25.9 ± 0.8 (−25.9)	−25.4–−25.4	−26.9–−24.5
Maple	2.7%	12	55.8 ± 8.8 (54.5)	62.6–62.6	36.7–69.2	12	−25.8 ± 2.6 (−25.4)	−23.9–−23.9	−29.9–−21.2
Alder	2.3%	10	60.7 ± 9.6 (59.8)	65.3–65.3	48.4–80.4	10	−25.5 ± 0.8 (−25.6)	−25.0–−25.0	−26.6–−24.1
Lime	1.6%	7	64.7 ± 15.1 (66.7)	67.8–67.8	35.7–87.1	7	−27.6 ± 1.9 (−28.3)	−25.7–−25.7	−30.1–−25.0

Birch	0.2%	1	48.3 ± 0.0 (48.3)	48.3–48.3	48.3–48.3	1	−24.3 ± 0.0 (−24.3)	−24.3–−24.3	−24.3–−24.3
Oak	3.4%	14	50.2 ± 16.8 (54.0)	61.6–61.6	15.8–73.4	14	−25.3 ± 2.1 (−25.7)	−24.2–−24.2	−27.8–−20.5
Beech	0.2%	1	57.3 ± 0.0 (57.3)	57.3–57.3	57.3–57.3	1	−28.1 ± 0.0 (−28.1)	−28.1–−28.1	−28.1–−28.1
Willow	0.2%	1	63.5 ± 0.0 (63.5)	63.5–63.5	63.5–63.5	1	−26.5 ± 0.0 (−26.5)	−26.5–−26.5	−26.5–−26.5
Plum	0.2%	1	58.8 ± 0.0 (58.8)	58.8–58.8	58.8–58.8	1	−26.5 ± 0.0 (−26.5)	−26.5–−26.5	−26.5–−26.5
Nutshell	1.1%	5	58.7 ± 8.5 (59.2)	64.7–64.7	47.6–69.8	5	−25.6 ± 0.7 (−25.6)	−25.1–−25.1	−26.4–−24.7
Unknown	0.2%	1	63.0 ± 0.0 (63.0)	63.0–63.0	63.0–63.0	1	−26.1 ± 0.0 (−26.1)	−26.1–−26.1	−26.1–−26.1
Hazel	0.7%	3	57.1 ± 11.4 (53.9)	65.8–65.8	47.6–69.8	3	−25.6 ± 0.9 (−25.6)	−24.9–−24.9	−26.4–−24.7
Oak	0.2%	1	59.2 ± 0.0 (59.2)	59.2–59.2	59.2–59.2	1	−25.3 ± 0.0 (−25.3)	−25.3–−25.3	−25.3–−25.3
Grain	0.2%	1	65.9 ± 0.0 (65.9)	65.9–65.9	65.9–65.9	1	−24.7 ± 0.0 (−24.7)	−24.7–−24.7	−24.7–−24.7
Barley	0.2%	1	65.9 ± 0.0 (65.9)	65.9–65.9	65.9–65.9	1	−24.7 ± 0.0 (−24.7)	−24.7–−24.7	−24.7–−24.7
Plant charred	0.2%	1	59.2 ± 0.0 (59.2)	59.2–59.2	59.2–59.2	1	−21.9 ± 0.0 (−21.9)	−21.9–−21.9	−21.9–−21.9
Common grape wine	0.2%	1	59.2 ± 0.0 (59.2)	59.2–59.2	59.2–59.2	1	−21.9 ± 0.0 (−21.9)	−21.9–−21.9	−21.9–−21.9

Wide ranges of $\delta^{13}C$ values can also be observed within one species (Table 1, Figure 3, Supplementary Figure 1). Calculating the averages of the wood and charcoal samples of the different species shows that there can be up to 2–3‰ differences between species (Table 1). For example, the species with the highest average $\delta^{13}C$ value is lime, with -26.3 ± 1.7‰ ($n = 4$), and the lowest is birch with -30.6 ± 2.7‰ ($n = 2$). Furthermore, Table 1, Figure 4E and Supplementary Figure 1 demonstrate again that in most cases, the charcoal is enriched in ^{13}C.

DISCUSSION

Wood consists of a variety of different chemical compounds, produced by different biochemical pathways. One could therefore hypothesize that part of the variability of the measured $\delta^{13}C$ values on wood are caused by the differential preservation of the different compounds, and that focusing on cellulose would reduce the variability. However, plant remains are reported to retain the original $\delta^{13}C$ signal after millennia (Metcalfe and Mead 2019). Furthermore, there is very little evidence that the variability in cellulose would be smaller, not even for individual trees of the same species growing under very similar conditions (McCarroll and Loader 2004). $\delta^{13}C$ variations have also been found within the cellulose of one single tree ring, e.g. seasonal variation of 1–2‰ between earlywood and latewood, or variation of 1–4‰ around the circumference of a tree ring (Francey and Farquhar 1982). Both charred and uncharred plant parts are reported to retain the original $\delta^{13}C$ signal, especially when an acid-base-acid pretreatment precedes the measurements (DeNiro and Hastorf 1985). Further, we observe no correlations between the $\delta^{13}C$ values and carbon content (%C) for any of the identified species (Supplementary Figure 1). Therefore, we are confident that the variability in our wood samples reflects the variability of the $\delta^{13}C$ values of the original wood.

In most species, the charcoal has less negative $\delta^{13}C$ values than the wood. This implies that either the most labile components of the wood are depleted in ^{13}C, or that generally the ^{13}C-depleted molecules are most easily lost during charring. As we find this $\delta^{13}C$-enrichment due to charring fairly consistently for different species and throughout time, this could indicate a general mechanism—in contrast to the literature, where both enrichment, depletion and unchanged $\delta^{13}C$ values are reported (see the Introduction and e.g. Ascough et al. 2008 for an overview). The nutshells of both species, hazel and oak, have intermediate $\delta^{13}C$ values between wood and charcoal (see Supplementary Figure 1).

One could expect that with such a large dataset, effects such as a climatic influence on the $\delta^{13}C$ values could be observed. Commonly $\delta^{13}C$ analysis of the cellulose fraction of tree rings is used for climate reconstruction (e.g. McCarroll and Loader 2004). However, significant correlations between the bulk wood and cellulose $\delta^{13}C$ values indicate the bulk wood values would be a good proxy for cellulose values, and they have both been found to correlate significantly with summer temperature and growing season precipitation (Hemming et al. 1998; Verheyden et al. 2005; Taylor et al. 2008; Mischel et al. 2015). Thus, one could speculate whether data like those presented in this study could be used for climate reconstruction as well. However, this would certainly require better temporal resolution, as we were not able to find any trends with time in our dataset (Figure 2). Furthermore, any long-term climatic trends could be hidden in the large $\delta^{13}C$ variation of the data. Charcoal $\delta^{13}C$ values were also proposed as a climate proxy (Ferrio et al. 2006). However, even though they are correlated to wood $\delta^{13}C$ values and were a useful proxy for aridity in the cited study, we

https://doi.org/10.1017/RDC.2019.138 Published online by Cambridge University Press

do not expect that trees in Denmark have been water-limited at any time in prehistory, and we have not found a long-term $\delta^{13}C$ trend in our charcoal or wood samples. However, climate reconstruction could be possible with tree-ring measurements of Danish trees, because correlations of $\delta^{13}C$ with ring width, temperature and precipitation have been found in Dutch trees, in a climate similar to the Danish climate (Francey and Farquhar 1982).

The time trends mentioned above in the Results section (see also Figure 2) cannot be explained by environmental or climatic factors alone, as we observe different trends for the two most dominant species, hazel and ash (Figure 2, panels C and D). The running mean of the hazel $\delta^{13}C$ values increases slightly between 5500 BP and 4500 BP, but no similar trend can be found in the other species, and we do not yet have an explanation for it. The $\delta^{13}C$ value of the ash sample peaks around 5000 BP, in contrast to the $\delta^{13}C$ values of other species (Figure 2 and Supplementary Figure 1). An explanation for this phenomenon might be found in the $\delta^{13}C$ differences between artifacts (spears and paddles) and non-artifacts (branches used in fish weirs)—the $\delta^{13}C$ values for artifacts are higher than those for non-artifacts (Supplementary Figure 2 and insert in Figure 2, panel D). In the time around 5000 BP, there was a peak in the ritual deposition of artifacts in shallow coastal water, including spears and paddles made of ash. Those were made of stems or older branches of ash, while the ash wood used for fish weirs was much younger, thus carrying a possible juvenile effect that could lower the $\delta^{13}C$ values. Furthermore, spears and paddles could have been produced elsewhere and been transported to the study region, carrying another region's isotope signature, while branches for fish weirs were most probably collected locally. Lev-Yadun et al. (2010) found, for a different environment, that imported wood could cause apparent $\delta^{13}C$ variations. The overall running mean of the wood $\delta^{13}C$ values decreases by about 2‰ after 6000 BP. This is probably caused by the different species analyzed here: the dataset before 6000 BP is dominated by oak and lime, which have comparatively high $\delta^{13}C$ values (Figure 3). After 6000 BP, hazel dominates the dataset and lowers the average wood $\delta^{13}C$ values as its $\delta^{13}C$ values are lower than those of oak and lime (Figure 3). This could indicate a changing environment due to the rising sea level, where an oak-dominated inland forest was replaced by a more open, hazel-dominated coastal woodland. However, the most probable explanation is the changing resource use by the prehistoric people: as the area turned into a coastal landscape, they started to build stationary fishing devices, primarily from hazel branches. Finally, the 2‰ drop after 6000 BP could also be a result of the small number of samples from this period. Ideally, more wood samples from around 6000 BP should be analyzed, also including hazel samples.

Although all samples come from an area that is ca. 2.5 km across at its maximum, the range of measured $\delta^{13}C$ values is as broad as that of other studies analysing samples from all over the world (e.g. Poole and Bergen 2006). Also, within one species, the range of $\delta^{13}C$ values was almost as large as that of our entire dataset. The same effect was observed by Van de Water et al. (2002), who found that individuals growing at the same site had the same degree of variability as plants along the entire altitudinal gradient. This could be due to the micro-environment in which the trunks and branches grew. For example, wood $\delta^{13}C$ values were observed to vary with sampling height within one individual tree, and whether the tree was shaded or exposed to sunlight (Wickman 1952; Li and Zhu 2011; McDowell et al. 2011). In dense forests, the CO_2 is ^{13}C-depleted compared to atmospheric CO_2. This mechanism is known as the canopy effect and has been observed both in trees and in herbivores, where tree samples from lower heights in dense forests and herbivore populations from dense forests have more depleted $\delta^{13}C$ values than those from open sites

https://doi.org/10.1017/RDC.2019.138 Published online by Cambridge University Press

(Vogel 1978; Medina and Minchin 1980; van der Merwe and Medina 1991; Noe-Nygård and Hede 2006; Drucker et al. 2008). Also, a juvenile effect, as explained in the introduction, could influence our $\delta^{13}C$ values. Therefore, we divided our samples into age groups and found that the youngest branches tend to have lower $\delta^{13}C$ values (Figure 3C). However, we were not able to distinguish young trees from young branches on old trees, which might explain the broad range of $\delta^{13}C$ values for the youngest group.

Our study site would have been ideal to show whether environmental changes have an effect on the $\delta^{13}C$ values of wood, because the rising sea level caused large changes in the gently sloping terrain. In spite of the substantial environmental changes at the study site, however, there are almost no temporal trends in our $\delta^{13}C$ data. The exception is a 2‰ increase in the average $\delta^{13}C$ values of wood samples from 6000 to 4200 BP. This corresponds to the period of strong relative sea level rise, as shown in Philippsen (2018: Fig. 4). One hypothesis to explain the increasing $\delta^{13}C$ could be the transition from a dense inland forest to a more open coastal forest, possible further opened up by human activity. Ongoing archaeological and palaeo-ecological research could answer this question in the future. Short-term fluctuations might be present in long series of individual tree rings, but we did not have the possibility to analyze them. This study could be improved further if samples from the same species had been available for the entire time range, or if all species had been represented by the same number as the dominating hazel.

Although there are differences in the average $\delta^{13}C$ values of the different species, their $\delta^{13}C$ ranges overlap to a large degree (Figures 3 and 4, Supplementary Figure 1). Therefore, the results of this study cannot be used to examine details in photosynthesis and plant physiology between different species. This would only be possible if there were significant differences between the species. Similar results have been observed in different cereal species, usually between 1‰ and 5‰ for one site (Hammers in prep., Fiorentino et al. 2012; Lightfoot and Stevens 2012; Bogaard et al. 2013; Kanstrup et al. 2014; Styring et al. 2016, 2017; Gron et al. 2017; Brinkkemper et al. 2018), although the ranges of those plants were not as broad as those in this study. This difference between our study and those cited above is remarkable, as one would expect a greater variability in a plant that is subjected to different cultivation and management practices, in addition to the natural variation that might be found in unmanaged plants.

The $\delta^{13}C$ values of plants are relevant for palaeodietary studies. On the one hand, plants were directly consumed by humans—not wood of course, but leaves, fruits, roots and tubers from plants. The broad $\delta^{13}C$ ranges of trees that were encountered in this study thus serve as a cautionary tale for establishing useful plant baseline isotopic values for palaeodietary reconstruction. The $\delta^{13}C$ values of edible plant parts could vary as much as those of our wood and charcoal samples. Furthermore, the foliage of the trees analyzed here could have served as fodder both for hunted animals as well as for domesticated animals. Although most of the variation found in the trees would have been averaged out in the transformation from plant to animal tissue (the average $\delta^{13}C$ value of a herbivore's total diet reflects the average of the plant $\delta^{13}C$ values of all plants consumed), it should be kept in mind that some of the variability might be transferred up the food chain. However, we cannot make direct comparisons between wood and foliage $\delta^{13}C$ values, as there can be considerable fractionation between wood and leaves. For example, Li and Zhu (2011) found that the leaves were enriched in $\delta^{13}C$ in comparison to the trunk and branches. In any case, isotope values of modern and archaeological tree samples are not directly comparable due to the $\delta^{13}C$ Suess effect (Suess 1955; Revelle and Suess 1957), but the

https://doi.org/10.1017/RDC.2019.138 Published online by Cambridge University Press

general fractionation trends will still be approximately the same. Therefore, although there might be deviations in the absolute values, we suggest that baseline data are collected for a broad range of plants for future palaeodietary studies.

CONCLUSION

In this study, we measured ^{14}C ages and $\delta^{13}C$ values on a total of 440 archaeological wood, charcoal and nutshell samples. We found that their $\delta^{13}C$ values span a range of more than 11‰. Also, within one single species, ranges of ca. 10‰ were observed. There is some variation in $\delta^{13}C$ values between different species, but the ranges overlap considerably (e.g., Table 1 and Figure 3). A general time-dependence of the $\delta^{13}C$ values was not observed for the study period (Figure 2). The results presented here show that large variations can be expected at the base of the food chain, which can add uncertainty to palaeodietary reconstructions. In the future, we will try to link the $\delta^{13}C$ values to the small-scale environment of where the tree grew—e.g., in a dense forest, one would expect lower $\delta^{13}C$ values than in an open woodland.

ACKNOWLEDGMENTS

We would like to thank all the archaeologists and technical staff from Museum Lolland-Falster for their support in the field and storage facilities, for their constant helpfulness and interest in scientific archaeology.

SUPPLEMENTARY MATERIAL

To view supplementary material for this article, please visit https://doi.org/10.1017/RDC.2019.138

REFERENCES

Ascough PL, Bird MI, Wormald P, Snape CE, Apperley D. 2008. Influence of production variables and starting material on charcoal stable isotopic and molecular characteristics. Geochimica et Cosmochimica Acta 72:6090–6102.

Beuning KRM, Scott JE. 2002. Effects of charring on the carbon isotopic composition of grass (Poaceae) epidermis. Palaeogeography, Palaeoclimatology, Palaeoecology 177:169–181.

Bogaard A, Fraser R, Heaton THE, Wallace M, Vaiglova P, Charles M, Jones G, Evershed RP, Styring AK, Andersen NH, Arbogast R-M, Bartosiewicz L, Gardeisen A, Kanstrup M, Maier U, Marinova E, Ninov L, Schäfer M, Stephan E. 2013. Crop manuring and intensive land management by Europe's first farmers, Proceedings of the National Academy of Sciences 110:12589–12594.

Brinkkemper P, Braadbaart F, van Os B, van Hoesel A, van Brussel AAN, Fernandes R. 2018. Effectiveness of different pre-treatments in recovering pre-burial isotopic ratios of charred plants. Rapid Communications in Mass Spectrometry 32:251–261.

Bronk Ramsey C. 2009. Bayesian analysis of radiocarbon dates. Radiocarbon 51(1):337–360.

Caracuta V, Weinstein-Evron M, Yeshurun R, Kaufman D, Tsatskin A, Boaretto E. 2016. Charred wood remains in the Natufian sequence of el-Wad terrace (Israel): New insights into the climatic, environmental and cultural changes at the end of the Pleistocene. Quaternary Science Reviews 131:20–32.

Craig H. 1953. The geochemistry of the stable carbon isotopes. Geochimica et Cosmochimica Acta 3(2–3): 53–92.

DeNiro MJ, Hastorf CA. 1985. Alteration of $^{15}N/^{14}N$ and $^{13}C/^{12}C$ ratios of plant matter during the initial stages of diagenesis: studies utilizing archaeological specimens from Peru. Geochimica et Cosmochimica Acta 49(1):97–115.

Drucker DG, Bridault A, Hobson KA, Szuma E, Bocherens H. 2008. Can carbon-13 in large herbivores reflect the canopy effect in temperate and boreal ecosystems? Evidence from modern and ancient ungulates. Palaeogeography, Palaeoclimatology, Palaeoecology 266(1):69–82.

Ferrio JP, Araus JL, Buxó R, Voltas J, Bort J. 2005. Water management practices and climate in ancient agriculture: inferences from the stable isotope composition of archaeobotanical

remains. Vegetation History and Archaeobotany 14(4):510–517.

Ferrio JP, Alonso N, López-Melción J, Araus J, Voltas J. 2006. Carbon isotope composition of fossil charcoal reveals aridity changes in the NW Mediterranean Basin. Global Change Biology 12(7):1253–1266.

Fiorentino G, Caracuta V, Casiello G, Longobardi F, Sacco A. 2012. Studying ancient crop provenance: implications from $\delta^{13}C$ and $\delta^{15}N$ values of charred barley in a Middle Bronze Age silo at Ebla (NW Syria). Rapid Communications in Mass Spectrometry 26:327–335.

Fiorentino G, Ferrio JP, Bogaard A, Araus J, Riehl S. 2014. Stable isotopes in archaeobotanical research. Vegetation History and Archaeobotany 24(1): 215–227.

Francey RJ, Farquhar GD. 1982. An explanation of $^{13}C/^{12}C$ variations in tree rings. Nature 297(5861): 28–31.

Gagen M, Zorita E, McCarroll D, Young GHF, Grudd H, Jalkanen R, Loader NJ, Robertson I, Kirchhefer A. 2011. Cloud response to summer temperatures in Fennoscandia over the last thousand years. Geophysical Research Letters 38(5):L05701.

Gron KL, Gröcke DR, Larsson M, Sørensen L, Larsson L, Rowley-Conwy P, Church MJ. 2017. Nitrogen isotope evidence for manuring of early Neolithic Funnel Beaker Culture cereals from Stensborg, Sweden. Journal of Archaeological Science: Reports 14:575–579.

Hafner P, Robertson I, McCarroll D, Loader NJ, Gagen M, Bale RJ, Jungner H, Sonninen E, Hilasvuori E, Levanic T. 2011. Climate signals in the ring widths and stable carbon, hydrogen and oxygen isotopic composition of *Larix decidua* growing at the forest limit in the southeastern European Alps. Trees – Structure and Function 25(6):1141–1154.

Hastorf CA, DeNiro MJ. 1985. Reconstruction of prehistoric plant production and cooking practices by a new isotopic method. Nature 315:489–491.

Heaton THE. 1999. Spatial, species, and temporal variations in the $^{13}C/^{12}C$ Ratios of C_3 plants: implications for palaeodiet studies. Journal of Archaeological Science 26(6):637–649.

Hemming DI, Switsur VR, Waterhouse JS, Heaton THE, Carter AHC. 1998. Climate variation and the stable carbon isotope composition of tree ring cellulose: an intercomparison of *Quercus robur*, *Fagus sylvatica* and *Pinus silvestris*. Tellus B: Chemical and Physical Meteorology 50(1):25–33.

Kanstrup M, Holst MK, Jensen PM, Thomsen IK, Christensen BT. 2014. Searching for long-term trends in prehistoric manuring practice. $\delta^{15}N$ analyses of charred cereal grains from the 4th to the 1st millennium BC, Journal of Archaeological Science 51:115–125.

Leavitt SW, Donahue DJ, Long A. 1982. Charcoal production from wood and cellulose: implications to radiocarbon dates and accelerator target production. Radiocarbon 24(1): 27–35.

Lev-Yadun S, Lucas DS, Weinstein-Evron M. 2010. Modeling the demands for wood by the inhabitants of Masada and for the Roman siege. Journal of Arid Environments 74(7): 777–785.

Li M, Zhu J. 2011. Variation of $\delta^{13}C$ of wood and foliage with canopy height differs between evergreen and deciduous species in a temperate forest. Plant Ecology 212(4):543–551.

Lightfoot E, Stevens RE. 2012. Stable isotope investigations of charred barley (*Hordeum vulgare*) and wheat (*Triticum spelta*) grains from Danebury Hillfort: implications for palaeodietary reconstructions, Journal of Archaeological Science 39:656–662.

Loader NJ, Santillo PM, Woodman-Ralph JP, Rolfe JE, Hall MA, Gagen M, Robertson I, Wilson R, Froyd CA, McCarroll D. 2008. Multiple stable isotopes from oak trees in southwestern Scotland and the potential for stable isotope dendroclimatology in maritime climatic regions. Chemical Geology 252(1–2): 62–71.

Marino BD, DeNiro MJ. 1987. Isotopic analysis of archaeobotanicals to reconstruct past climates: Effects of activities associated with food preparation on carbon, hydrogen and oxygen isotope ratios of plant cellulose. Journal of Archaeological Science 14(5):537–548.

McCarroll D, Loader NJ. 2004. Stable isotopes in tree rings. Quaternary Science Reviews 23(7):771–801.

McDowell NG, Bond BJ, Dickman LT, Ryan MG, Whitehead D. 2011. Relationships between tree height and carbon isotope discrimination. In: Meinzer FC, Lachenbruch B, Dawson T, editors. Size- and age-related changes in tree structure and function: Springer. p 255–286.

Medina E, Minchin PEH. 1980. Stratification of $\delta^{13}C$ values of leaves in Amazonian rain forests. Oecologia 45(3):377–378.

Metcalfe JZ, Mead JI. 2019. Do uncharred plants preserve original carbon and nitrogen isotope compositions? Journal of Archaeological Method and Theory 26(2):844–872.

Mischel M, Esper J, Keppler F, Greule M, Werner W. 2015. $\delta^{2}H$, $\delta^{13}C$ and $\delta^{18}O$ from whole wood, α-cellulose and lignin methoxyl groups in *Pinus sylvestris*: a multi-parameter approach. Isotopes in Environmental and Health Studies 51(4): 553–568.

Noe-Nygård N, Hede MU. 2006. The first appearance of cattle in Denmark occurred 6000 years ago: an effect of cultural or climate and environmental changes. Geografiska Annaler, Series A Physical Geography 88(2): 87–95.

Olsen J, Tikhomirov D, Grosen C, Heinemeier J, Klein M. 2016. Radiocarbon analysis on the new AARAMS 1MV Tandetron. Radiocarbon 59:905–913.

Park R, Epstein S. 1960. Carbon isotope fractionation during photosynthesis. Geochimica et Cosmochimica Acta 21(1):110–126.

Philippsen B. 2018. Reservoir effects in a Stone Age Fjord on Lolland, Denmark. Radiocarbon 60(2): 653–665.

Poole I, Bergen PFv. 2006. Physiognomic and chemical characters in wood as palaeoclimate proxies. Plant Ecology 182(1):175–195.

Reimer PJ, Bard E, Bayliss A, Beck JW, Blackwell PG, Bronk Ramsey C, Buck CE, Cheng H, Edwards RL, Friedrich M, Grootes PM, Guilderson TP, Haflidason H, Hajdas I, Hatté C, Heaton TJ, Hoffmann DL, Hogg AG, Hughen KA, Kaiser KF, Kromer B, Manning SW, Niu M, Reimer RW, Richards DA, Scott EM, Southon JR, Staff RA, Turney CSM, van der Plicht J. 2013. IntCal13 and Marine13 radiocarbon age calibration curves 0–50,000 years cal BP. Radiocarbon 55(4):1869–1887.

Revelle R, Suess HE. 1957. Carbon dioxide exchange between atmosphere and ocean and the question of an increase of atmospheric CO_2 during the past decades. Tellus IX:18–27.

Santos GM, Southon JR, Griffin S, Beaupre SR, Druffel ERM. 2007. Ultra small-mass AMS ^{14}C sample preparation and analyses at KCCAMS/UCI Facility. Nuclear Instruments & Methods in Physics Research B 259:293–302.

Stuiver M, Braziunas TF. 1987. Tree cellulose $^{13}C/^{12}C$ isotope ratios and climatic change. Nature 328(6125):58–60.

Stuiver M, Polach HA. 1977. Discussion: Reporting of ^{14}C data. Radiocarbon 19(3):355–363.

Suess HE. 1955. Radiocarbon Concentration in Modern Wood. Science 122(3166):415–417.

Sørensen SA. 2016. Denmark's largest Stone Age excavation. Mesolithic Miscellany 24(2):3–10.

Styring A, Ater M, Hmimsa Y, Fraser R, Miller H, Neef R, Pearson JA, Bogaard A. 2016. Disentangling the effect of farming practice from aridity on crop stable isotope values: A present-day model from Morocco and its application to early farming sites in the eastern Mediterranean. The Anthropocene Review 3:2–22.

Styring AK, Charles M, Fantone F, Hald MM, McMahon A, Meadow RH, Nicholls GK, Patel AK, Pitre MC, Smith A, Soltysiak A, Stein G, Weber JA, Weiss H, Bogaard A. 2017. Isotope evidence for agricultural extensification reveals how the world's first cities were fed. Nature Plants 3:1–11.

Taylor AM, Brooks JR, Lachenbruch B, Morrell JJ, Voelker S. 2008. Correlation of carbon isotope ratios in the cellulose and wood extractives of Douglas-fir. Dendrochronologia 26:1251–31.

Turekian VC, Macko S, Ballentine D, Swap R, Garstang M. 1998. Causes of bulk carbon and nitrogen isotopic fractionations in the products of vegetation burns: Laboratory studies. Chemical Geology 152(1–2):181–192.

Van de Water PK, Leavitt SW, Betancourt JL. 2002. Leaf $\delta^{13}C$ variability with elevation, slope aspect, and precipitation in the Southwest United States. Oecologia 132(3):332–343.

van der Merwe NJ, Medina E. 1991. The canopy effect, carbon isotope ratios and foodwebs in Amazonia. Journal of Archaeological Science 18(3):249–259.

Verheyden A, Roggeman M, Bouillon S, Elskens M, Beeckman H, Koedam N. 2005. Comparison between $\delta^{13}C$ of α-cellulose and bulk wood in the mangrove tree *Rhizophora mucronata*: Implications for dendrochemistry. Chemical Geology 219(1):275–282.

Vignola C, Masi A, Balossi Restelli F, Frangipane M, Marzaioli F, Passariello I, Rubino M, Terrasi F, Sadori L. 2018. $\delta^{13}C$ values in archaeological ^{14}C-AMS dated charcoals: Assessing mid-Holocene climate fluctuations and human response from a high-resolution isotope record (Arslantepe, Turkey). Rapid Communications in Mass Spectrometry 32:1149–1162.

Vogel JC. 1978. Recycling of CO_2 in a forest environment. Oecologia Plantarum 13:89–94.

Vogel JS, Southon JR, Nelson DE, Brown TA. 1984. Performance of catalytically condensed carbon for use in accelerator mass spectrometry. Nuclear Instruments and Methods in Physics Research Section B: Beam Interactions with Materials and Atoms 5(2):289–293.

Wickman FE. 1952. Variations in the relative abundance of the carbon isotopes in plants. Geochimica et Cosmochimica Acta 2(4): 243–254.

Young GHF, McCarroll D, Loader NJ, Kirchhefer AJ. 2010. A 500-year record of summer near-ground solar radiation from tree-ring stable carbon isotopes. Holocene 20(3):315–324.

Young GHF, Bale RJ, Loader NJ, McCarroll D, Nayling N, Vousden N. 2012a. Central England temperature since AD 1850: the potential of stable carbon isotopes in British oak trees to reconstruct past summer temperatures. Journal of Quaternary Science 27(6):606–614.

Young GHF, McCarroll D, Loader NJ, Gagen MH, Kirchhefer AJ, Demmler JC. 2012b. Changes in atmospheric circulation and the Arctic Oscillation preserved within a millennial length reconstruction of summer cloud cover from northern Fennoscandia. Climate Dynamics 39(1–2): 495–507.